

# Long Duration Testing of a Spacesuit Water Membrane Evaporator Prototype

Grant C. Bue<sup>1</sup>, Janice Makinen<sup>2</sup>, Marlon Cox<sup>3</sup>, Carly Watts<sup>4</sup> and Colin Campbell<sup>5</sup>  
*NASA Johnson Space Center, Houston, TX, 77058*

*and*

Matthew Vogel<sup>6</sup>, Aaron Colunga<sup>7</sup> and Bruce Conger<sup>8</sup>  
*Jacobs Engineering, Engineering and Science Contract Group, Houston, TX, 77058*

The Spacesuit Water Membrane Evaporator (SWME) is a heat-rejection device that is being developed to perform thermal control for advanced spacesuits. Cooling is achieved by circulating water from the liquid cooling garment (LCG) through hollow fibers (HoFi's), which are small hydrophobic tubes. Liquid water remains within the hydrophobic tubes, but water vapor is exhausted to space, thereby removing heat. A SWME test article was tested over the course of a year, for a total of 600 cumulative hours. In order to evaluate SWME tolerance to contamination due to constituents caused by distillation processes, these constituents were allowed to accumulate in the water as evaporation occurred. A test article was tested over the course of a year for a total of 600 cumulative hours. The heat rejection performance of the SWME degraded significantly--below 700 W, attributable to the accumulation of rust in the circulating loop and biofilm growth. Bubble elimination capability, a feature that was previously proven with SWME, was compromised during the test, most likely due to loss of hydrophobic properties of the hollow fibers. The utilization of water for heat rejection was shown not to be dependent on test article, life cycle, heat rejection rate, or freezing of the membranes.

## Nomenclature

EVA	=	extravehicular activity
GN <sub>2</sub>	=	gaseous nitrogen
HoFi	=	hollow fiber
ISS	=	International Space Station
JSC	=	Johnson Space Center
PLSS	=	portable life support subsystem
SWME	=	suit water membrane evaporator

## I. Introduction

Thermal control of the crew during extravehicular activities (EVA) using the NASA Space Shuttle/International Space Station Extravehicular Mobility Unit (EMU) is provided by flowing chilled water through the spacesuit

---

<sup>1</sup> Aerospace Technologist, 2101 NASA Parkway, Houston, TX, 77058, Mail Stop EC2, nonmember

<sup>2</sup> Aerospace Technologist, 2101 NASA Parkway, Houston, TX, 77058, Mail Stop EC2, nonmember

<sup>3</sup> Aerospace Technologist, 2101 NASA Parkway, Houston, TX, 77058, Mail Stop EC5, nonmember

<sup>4</sup> Aerospace Technologist, 2101 NASA Parkway, Houston, TX, 77058, Mail Stop EC5, nonmember

<sup>5</sup> Aerospace Technologist, 2101 NASA Parkway, Houston, TX, 77058, Mail Stop EC5, nonmember

<sup>6</sup> Thermal Analyst, 2224 Bay Area Blvd., Houston, TX, 77058, Mail Stop JE-5EA, member

<sup>7</sup> Mechanical Engineer, 2224 Bay Area Blvd., Houston, TX, 77058, Mail Stop JE-5EA, nonmember

liquid cooling garment that wraps around the crew torso, arms and legs and picks up crew heat. The warm water is then pumped to the EMU Portable Life Support System (PLSS) sublimator heat exchanger where it is cooled by sublimation of ice that is continually supplied with water from a separate water tank. While the current EMU PLSS sublimator has been very successful, its limitations and anticipated future PLSS requirements have motivated investigations of alternate means to provide cooling to the space-suited crew. One promising alternative is the spacesuit water membrane evaporator (SWME) in which the flowing water coolant is directly cooled through evaporation of a small fraction of the flowing water.

The HoFi SWME long duration testing detailed in this paper represents another step in a multi-year effort to develop HoFi SWME technology. The test article is the second generation (Gen2) HoFi SWME that is fundamentally the same as the first generation (Gen1) HoFi SWME. Both generations packaged approximately 14900 hydrophobic, porous hollow fibers into a cylindrical housing to form the core of the SWME heat rejection device. In addition, both generations used a backpressure valve to throttle the heat rejection as needed. Differences between the first and second generations lie in the Gen2 efforts to lower total mass, ease cartridge change-out, and integrate the backpressure valve while meeting the same heat rejection and water pressure drop performance requirements.

Gen2 HoFi SWME testing was performed in Building 220 at NASA-Johnson Space Center using the Chamber R vacuum chamber and part of the PLSS 1.0 test rig. Buildup of the Gen2 HoFi SWME test loop occurred in parallel with the buildup of the PLSS 1.0 test rig since the SWME test loop comprised the PLSS 1.0 Thermal Loop. Stand alone Gen2 HoFi SWME testing, in which the other PLSS loops were not operated, was conducted from 11 March to 9 May 2011, much of which was reported in a previous paper.<sup>1</sup> This paper reports follow-on stand-alone and integrated PLSS 1.0 testing that continued through 30 September where performance, de-bubbling, freeze testing and feedwater utilization were revisited.

## II. Overview of Test Articles

Figure 1 presents a photograph of a Gen2 HoFi SWME test article with several key components identified including the fiber cartridge, housing, and backpressure valve (BPV) assembly. A cross-sectional and functional schematic of the Gen2 HoFi SWME is also presented in **Error! Reference source not found.** (on right) and illustrates the basic SWME operation in which entering warm water is cooled as it flows through the fiber cartridge and exiting water vapor is ported through the BPV. Direct evaporation of the water coolant is possible through hydrophobic porous membranes. Liquid water flowing through the channel formed by the membrane is prevented from flowing across the membrane porous walls due to its hydrophobic nature. Evaporative cooling of the water occurs when the water vapor pressure at the channel outside wall is lower than the water saturation pressure at the membrane inner wall. This vapor pressure difference permits water at the membrane inner wall to boil off with the vapor then flowing through the membrane porous walls. The evaporation rate increases substantially when the total gas pressure at the membrane outside wall is lower than the water saturation pressure at the membrane inner wall.

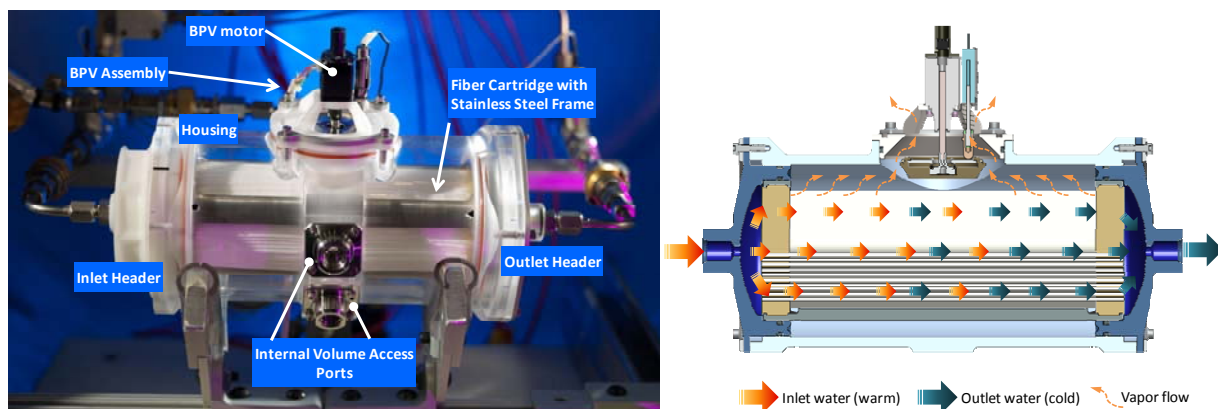


**Figure 1 Gen2 HoFi SWME Key Components and Function**

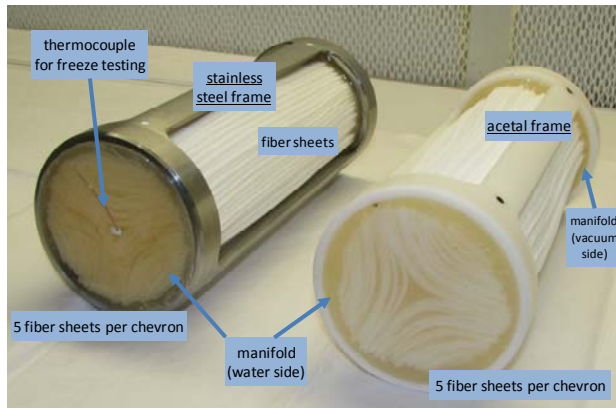


**Figure 2 Stainless Steel and Acetal Framed Fiber Cartridges (both 14900 fiber count)**

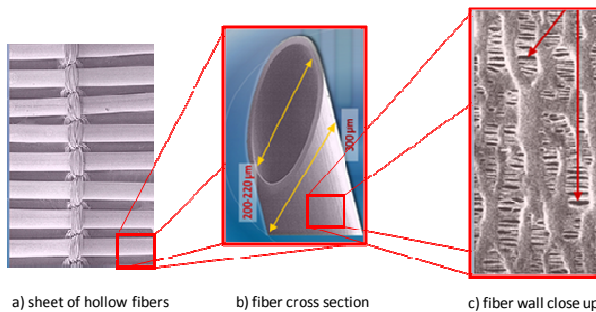
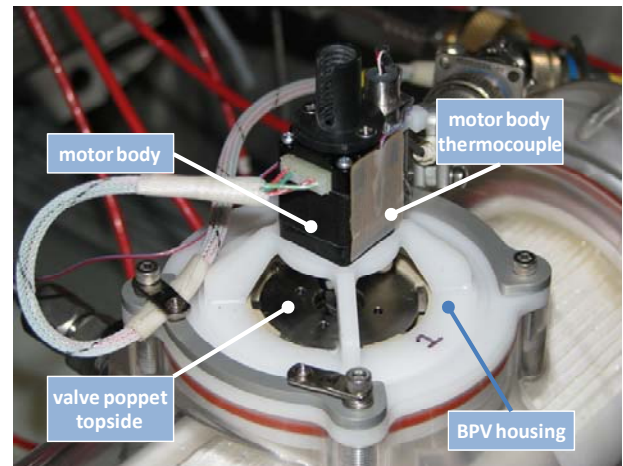


**Figure 3 Photos of the Celgard X50-215 Microporous Hollow Fiber Membrane**

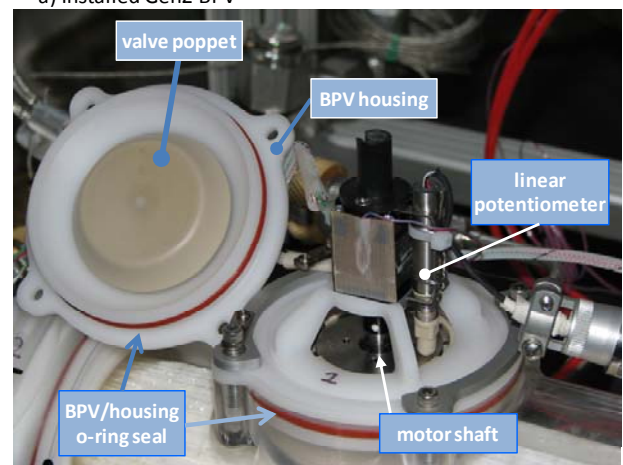
The Celgard X50-215 microporous hollow fiber membrane used in these test articles has nominal dimensions of 220 µm inner diameter, 40 µm wall thickness, 40% wall porosity, and 0.04 µm effective pore size. The average sheet fiber density is 21 fibers per centimeter (see Figure 3). A copy of the Celgard X50-215 membrane datasheet is placed in Appendix B for reference since it currently cannot be located on the manufacturer website.

**Error! Reference source not found.** presents two photos of the backpressure valve (BPV). Main BPV components are the motor, poppet, and housing. The motor selected for the Gen2 HoFi SWME BPV is a stepper motor that extends and retracts its shaft a total of 12.7 mm at a rate of 0.00305 mm per step. Around 4170 steps are required to fully extend or retract the motor shaft. Connected to the motor shaft is the poppet, which seats against the valve housing underside when closed. The motor shaft extension moves the valve poppet away from the housing and opens the annular valve throat. The maximum throat area is 1290 mm<sup>2</sup>. The BPV housing includes the quad leg frame which mounts the motor and seal for the BPV housing-SWME housing interface. A linear potentiometer was attached to the BPV to measure the poppet travel. The thermocouple measured the valve motor body temperature during testing.

For this technology development effort, two fiber cartridges were fabricated with 316 series stainless steel frames while two others were fabricated with DuPont Delrin 511P acetal plastic frames (see Figure 2). The fiber sheets were folded into 30 nested chevron shapes. Three of the cartridges contained five sheets per chevron resulting in a total of 14900 fibers. The remaining stainless steel framed fiber cartridges was assembled with six sheets per chevron resulting in a total of ~17900 fibers. This stainless steel cartridge initially leaked and was repaired using polyurethane. Approximately 1.7% of its 17900 fibers were blocked as a result of the repair process. One of the acetal cartridge fiber assemblies served as the prime test article for long duration testing.



a) Installed Gen2 BPV



b) Poppet and Potentiometer View

**Figure 4 Gen2 HoFi SWME Backpressure Valve**

### III. Test Methods

All Gen2 HoFi SWME testing was performed in Building 220 at NASA JSC with the SWME installed in the Chamber R vacuum chamber. Figure 5 presents the PLSS 1.0 test rig of which the Gen2 HoFi SWME was a component. During the first stage of SWME testing, only the PLSS 1.0 Thermal Loop was operational, thus permitting independent SWME testing. The second stage of SWME testing was performed as part of the PLSS 1.0 test program in which the Oxygen and Ventilation Loop Systems were operational. The data acquisition and control system (DACS) was based on National Instruments LabVIEW software code that operated on a dedicated personal computer platform. The DACS also controlled the SWME BPV through one of several LabVIEW modules written by project engineers for this test.

#### A. Test Setup

**Error! Reference source not found.** presents a schematic of the PLSS 1.0 Thermal Loop identifying key components and instrumentation. Thermal Loop heat sources representing the avionics and crew heat loads conditioned the water entering the SWME and were located immediately before and after the SWME, respectively. The crew heat sources were part of the Liquid Cooling Ventilation Garment (LCVG) simulator and consisted of a 1000 W heater and heat exchanger that transferred heat from/to a chiller cart via a separate water loop. A commercial-off-the-shelf variable speed pump generated required water flow around the Thermal Loop. Makeup water was supplied from the Feedwater System simulator.

#### B. Key Instrumentation

Key instrumentation with respect to SWME performance measurements included the immersed thermistors before and after the SWME, vapor backpressure sensor, water flow meters, and makeup water mass scale. Calculations of SWME heat rejections

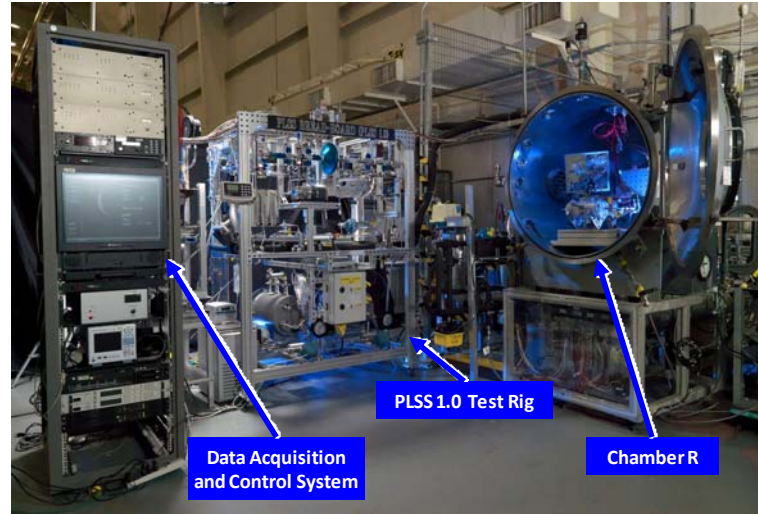


**Figure 5 Overview of PLSS 1.0 Test Configuration with Gen2 HoFi SWME in Chamber R**

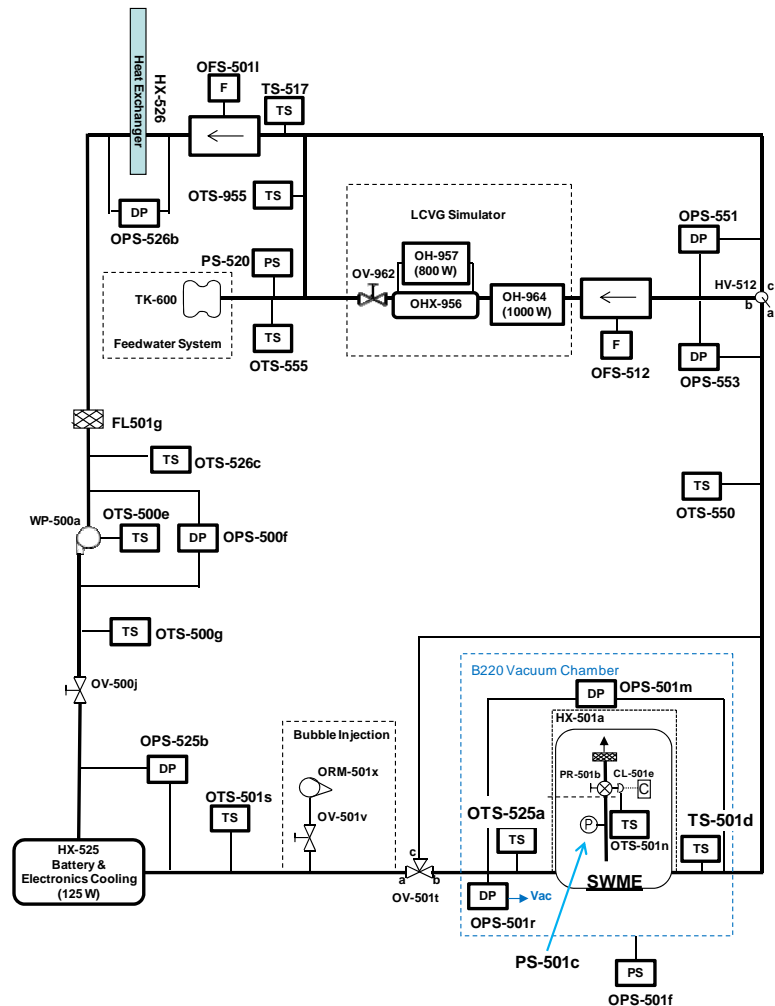


**Figure 6 Schematic of PLSS 1.0 Thermal Loop**



and instantaneous vapor mass flow rates were based on being able to accurately measure mass flow and temperatures. Inlet and outlet temperatures were measured with Fluke Hart Scientific 5611T thermistor probes that have a  $\pm 0.01^\circ\text{C}$  accuracy. Thermistor sensors were monitored by the Fluke Hart Scientific Black Stack Model 1560 thermometer via its Fluke Hart Scientific Model 2564 thermistor scanner. These components have an accuracy of  $\pm 0.003^\circ\text{C}$ , better than the thermistors themselves. The temperature instrumentation accuracy in terms of SWME heat rejection at 91 kg/hr water flow is  $\pm 1.4$  W. The Micromotion ELITE Peak Performance coriolis flow meter (model CMF025) has an accuracy of 0.05% of measured value. Assuming accurate temperatures, then the water flow rate measurements accuracy yields heat rejection rates accurate to within 0.05 W/K. SWME backpressures were measured by a Baratron 690A 100 mmHg series, which has a worst case accuracy of 0.12% of reading. The makeup water mass measurements were performed using an Arlyn Scales Saw-H Ultra Precision 100 kg capacity scale with an accuracy of 0.005%. Measurements of water used during testing provide a way to correlate mean SWME heat rejection rates.

### C. Long Duration Tests

The long duration test series was designed to determine sensitivity of the HoFi SWME element to ordinary constituents that are expected to be found in the potable water source. Water constituent levels were determined based on long-term performance of the International Space Station (ISS) water processing assembly and concentration of those impurities were multiplied by a factor of 2 to 5 for the test loop water.<sup>1</sup> While these levels are more concentrated than those found in ISS potable water, they are well below the limits set by NASA for human consumption. This worst-case potable water was selected as the baseline water quality to be supplied to the feedwater tank (Table 1). Some ordinary potable water impurities (e.g., organics) are volatile while others (e.g., metals and inorganic ions) are more or less nonvolatile. The nonvolatile constituents are expected to concentrate in the HoFi SWME as evaporated water from the loop is replaced by the feedwater. At some point in the HoFi SWME mission life cycle, as the concentrations of the nonvolatile impurities increase, solubility limits of one or more of the constituents may be reached. The resulting presence of precipitate in the coolant water may begin to plug pores and tube channels, ultimately affecting HoFi SWME performance..

Unlike previous contamination testing in which contaminant concentrations found in Table 1 were conservatively projected to simulate contaminated water for specific levels (e.g., 0, 33, 66 and 100 EVAs<sup>3-7</sup>), the philosophy of this test series to date (0-76 days) and future test series (76-100 days and beyond) is to accumulate contaminants in a flight-like manner. The heat-rejection rates for most of these test days exceeded the expected EVA average.

Metals testing, ion chromatography testing, total organic carbon testing, and bacterial colony-forming units were assayed every 5 test days.

**Table 1. SWME Feedwater**

ITEM	Amount (mg/L)
<b>Chemical</b>	
Barium	0.1
Calcium	1
Chlorine	5
Chromium	0.05
Copper	0.5
Iron	0.2
Lead	0.05
Magnesium	1
Manganese	0.05
Nickel	0.05
Nitrate	1
Potassium	5
Sulfate	5
Zinc	0.5
<b>Organic Constituents</b>	
Total Acids	0.5
Total Alcohols	0.5
Total Organic Carbon	0.3

### D. Bubble Tests

Bubble performance tests had been analyzed with the Gen2 SWME at day 24 and shown to eliminate all air bubbles, include 8 liters of air bubbles delivered over a 30 minute period.<sup>1</sup> In these tests air bubbles were streamed into the sample port while performance was monitored. Clear tubing segments allowed viewing of the inlet and outlet coolant streams to verify the presence of circulating bubbles. None had been observed. At day 57, bubble tests were repeated to see if bubbling capability was still retained. In these tests 60 cc of air bubbles were into the sample port. The pressure of the system was varied in 2 psi increments from 0 to 10 psig. The flow rate was tested at 91 kg/hr and 156 kg/hr. Both a long duration and an unused cartridge were tested.

### E. Extreme Freeze Test

Freeze tests analyzed Gen2 SWME vulnerability to freezing conditions. Previous intermittent freeze tests, water flow was stopped for 15 min and 30 min while keeping the backpressure valve open to freeze water contained in the water passages.<sup>1-3</sup> The valve was closed after the freeze period. When the membranes thawed, the pump was

gradually turned back on and the Gen2 SWME was inspected for leaks and other damage indications due to ice formation.

A long-duration freeze test was conducted with the Stainless Steel 14900-fiber unused cartridge, to protect the prime test article. The housing was wrapped with multilayer insulation to limit heat leak. For the extreme freeze test, the Gen2 SWME was fitted with 8 thermocouples, see Table 2.

In an extended freeze test, the Gen2 SWME back-pressure valve was fully opened and the water flow to the inlet halted for 1 hrs. After 1 hrs, the backpressure valve was closed and the unit was allowed to thaw. This required a repressurization/depressurization cycle to remove the multilayer insulation. Once thawed, the pump was turned back on, and the performance was monitored.

#### Back Pressure Valve Characterization

The initial backpressure valve (BPV) characterization test was performed on March 25, 2011 with a partial repeat performed on March 29, 2011. The BPV was stepped down in 28 discrete positions from a fully open position to a fully closed position. These 28 BPV positions, corresponds to a predetermined BPV valve throat area and, therefore, valve poppet linear travel, the goal to effect 30 W SWME heat rejection change from one position to the next.

## F. Utilization Tests

The utilization is a measure of efficiency and is equal to the ratio of apparent water consumption calculated from heat rejection to independent mass measurements of water used. The SWME heat rejection is integrated with respect to time and then divided by the water latent heat of vaporization to yield mass of water evaporated. Ideally the SWME utilization is 1 which would show that all water consumed resulted in measured heat rejection.

In order to quantify the efficiency of the SWME as a heat rejection device, utilization was calculated for different aspects of interest of SWME operation. Utilization calculations are based on SWME heat rejection calculations and water usage measurements, which were monitored throughout the entire test using a highly accurate precision scale.

**Table 2. Extended Freeze Test Temperature Sensor Placement**

Temperature Sensor Descriptor	Temperature Measured	Sensor Type	Notes
SWME Inlet T	Water	Thermistor	located in fluid line ~150 mm upstream of SWME
SWME Outlet T	Water	Thermistor	located in fluid line ~150 mm downstream of SWME
Mid, Radial Outer	Fiber	Type T thermocouple	Glued to outer wall of fiber located at perimeter of axial middle section
Mid, Radial Center	Fiber	Type T thermocouple	Glued to outer wall of fiber located at center of axial middle section
Outlet, Radial Outer	Fiber	Type T thermocouple	Glued to outer wall of fiber located at perimeter, outlet section just before the outlet polyurethane manifold
Outlet, Radial Center	Fiber	Type T thermocouple	Glued to outer wall of fiber located at center, outlet section just before the outlet polyurethane manifold
Inlet in PU	Polyurethane manifold	Type T thermocouple	Glued to the center, water side of inlet polyurethane manifold (see Figure 2)
Inlet Water	Inlet Header Water	Type T thermocouple	Placed about 6 mm away from water side of the inlet manifold
Outlet in PU	Polyurethane manifold	Type T thermocouple	Glued to the center, water side of outlet polyurethane manifold (see Figure 2)
Outlet Water	Outlet Header Water	Type T thermocouple	Placed about 6 mm away from water side of the outlet manifold

## IV. Results

### A. Long Duration Performance

The long duration performance test series is meant to gauge the long term HoFi SWME performance. Each test point represents fully open BPV, 91 kg/hr inlet water flow heat rejection measurements of the acetal cartridge SWME, with a 10 °C outlet temperature. Results from Day 0, March 11, to Day 73, September 23, are plotted in **Error! Reference source not found..** Based on previous undocumented test observations, the significant drop after the break-in day, Day 0, was expected as was the post-freeze test heat rejection increase. The magnitude of the post-freeze test heat rejection increases (>100 W) did, however, prove surprising. The post-freeze test response is believed to be the result of ice inside the hollow fibers stretching the fibers. This ice induced stretching could cause increased heat rejections by increasing the fiber diameter and, thus, active surface area and also by reducing the wall thickness. The downward heat rejection trends subsequent to the post-freeze upward spikes suggest the freeze effect is temporary.

From April 7 to May 4, the last segment of SWME stand alone testing, the acetal cartridge HoFi SWME heat rejection ranged from 815 to 855 W. After the SWME was not used for a month, its heat rejection dropped to 750 W at the beginning of integrated PLSS testing. From that point and onward the fully open BPV, 10 °C outlet water heat rejection ranged from 680 to 755 W. The first sub 700 W heat rejection decrease (23 June) is attributable to biofilms and contaminants plugging fiber inlets. Wetted surfaces of fittings in the loop had coatings consistent with biofilm. At the same time an increase in reddish-brown deposits were observed, coincident with pressure drop increases across the SWME and filters. Analysis of these deposits were consistent with corrosion products of non-passivated stainless steel and brazed components, both of which were present in the PLSS 1.0 coolant loop. The

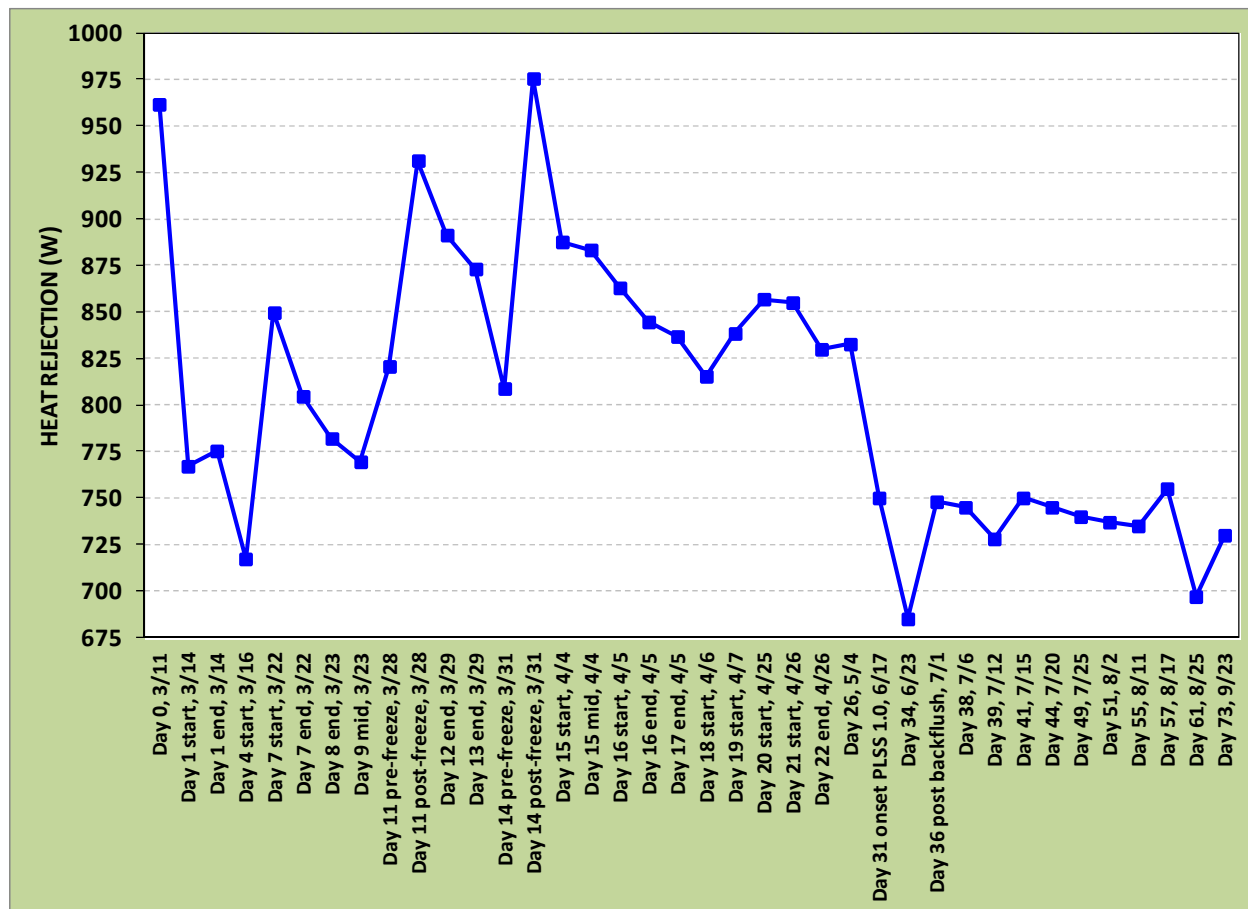


**Figure 7. Gen2 baseline performance through 73 days of testing**

presence of iron, chrome, nickel and oxygen are found on the residue of a system filter that underwent a Scanning Electron Microscope Energy Dispersive Spectrum analysis and is indicative of stainless steel corrosion products.<sup>8</sup> Of the two alloys of stainless steel intended for use in the wetted loop (304L and 316L), 304L would be expected to be less corrosion resistant and a more likely source of the corrosion products. COTS parts containing pump shafts, QDs, pressure transducers and manual valves tend to contain less corrosion resistant stainless steels (15-5 PH and 17-4 PH) and could not be ruled out as sources of the stainless steel corrosion products at the time of this writing.

The SWME was removed from the water loop and back flushed and then reinserted into the water loop. Subsequent performance was around 750 W. The cause of the second step down below 700 W is not fully understood. However, the usual suspects of microbial growth and corrosion contaminants cannot be ruled out.

## B. Repeat Bubble Tests

At test day 51, about three months after the first bubble test series, bubbles had been observed entering and exiting the SWME without appreciably vented through the fiber pores to the vacuum chamber. At test day 57 a series of bubble tests of 0.06 L each were conducted to determine the conditions in which the prime test cartridge could eliminate bubbles, if any. The test trials are listed in Table 3 in order of decreasing challenge for bubble elimination, to find out under what condition de-bubbling capability remained. Higher gauge pressures, and lower

flow rates would help to drive bubbles out through the pores. But the long duration test article had clearly lost this capability, even at 68.7 kPa gauge pressure. There was speculation that the introduction of a filter into the cooling loop reduced the gauge pressure of the SWME and affected bubble size and may thereby may have impacted the de-bubbling capability. However, many of the test points were repeated without an upstream filter, but the results were the same. When the long duration membrane cartridge was replaced with a pristine cartridge, one that had only previously been tested for leaks, it was found, at 0 kPa and 34.3 kPa gauge pressure, all bubbles were eliminated as in the earlier test. The ordinary mechanism for bubble elimination suggests why the de-bubbling capability is lost with fouling. As an air bubble enters a pristine fiber channel, the air would readily displace the water from the hydrophobic membrane surface, and the surface tension defining the bubble boundary is thereby relieved and the bubble is effectively broken, venting out the pores. Whereas the cycled long duration cartridge has apparently lost hydrophobicity either through accumulation of biofilm or corrosion contaminants or both. Outer portions of the long cycled membrane pores apparently remain hydrophobic, otherwise the cycled fibers would leak profusely, although some droplets had been observe to seep through some of the pores and collect on the outside surfaces of the membranes. However the inner regions appear to have become progressively become hydrophilic. With the interior of the fiber channel thus transformed, the bubble would travel through the tube without coming into contact with a sufficiently hydrophobic membrane because the high surface tension at the margins of the 0.04  $\mu\text{m}$  pores would restrain the bubble from entering the pores and reaching a hydrophobic region of the pore channel.

As compromised as the long duration cartridge had become for de-bubbling, it is safe to assume that just as the long duration cartridge retained the bulk of its evaporation capability (see Figure 7), it has not its ability to degas dissolved gases.

### C. Extreme Freeze Test

With coolant flow stopped the BPV was opened fully to sub cool the fibers below freezing until the manifold polyurethane and manifold coolant reached freezing. The SWME configuration was wrapped with aluminized Mylar to ensure minimal environmental heat loading, and promote rapid cooling.

Test results from the long duration freeze test presented in **Error! Reference source not found.** show that the water side of the inlet and outlet polyurethane manifolds reached freezing at 1.47 and 1.51 hours of elapsed test time. Time for the water side of the manifolds

to reach freezing ranged from 52 to 55 minutes after pump shut down. The manifold polyurethane temperatures tracked each other after the onset of freezing and reached a transient minimum of -1  $^{\circ}\text{C}$  at 1.8 hours of elapsed test

**Table 3. Bubble Test Revisited at 57 test days**

Chamber Pressure	Coolant Flow kg/hr	Gauge Pressure kPa (psig)	Bubbles Eliminated? Test Article	
			57 EVA	Pristine
Ambient	91	0.0 (0.0)	n	y
Ambient	91	13.7 (2.0)	n	
Ambient	91	27.5 (4.0)	n	
Ambient	91	34.3 (5.0)		y
Ambient	91	41.2 (6.0)	n	
Ambient	91	54.9 (8.0)	n	
Ambient	156	68.7 (10.0)	n	
Ambient	91	68.7 (10.0)	n	
22 Pa	91	68.7 (10.0)	n	

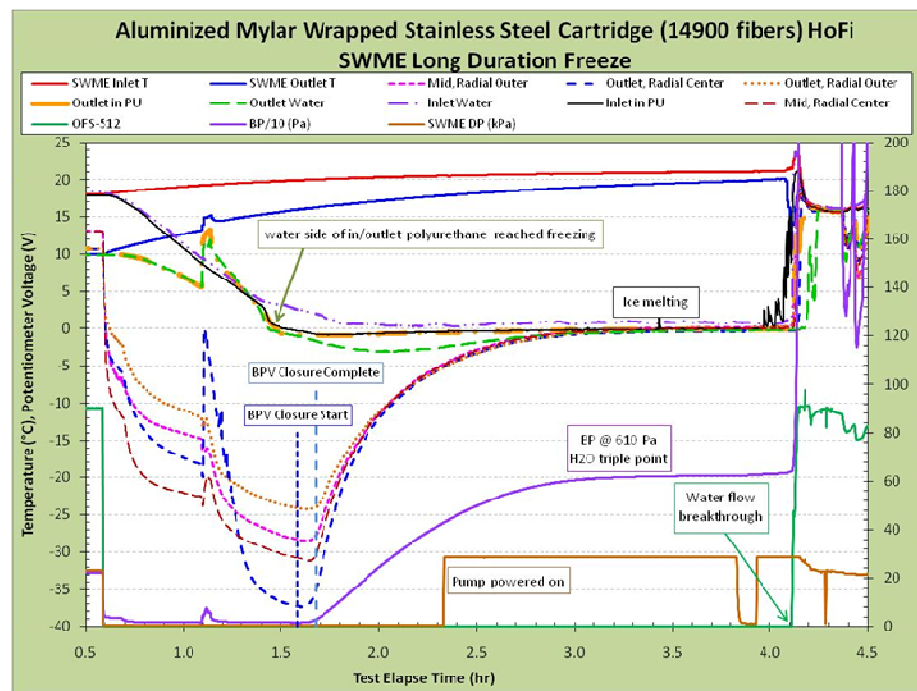


**Figure 8. 1-Hour Freeze Test**



time, about 6 minutes after the BPV closure completed. The temperature spikes that occurred at 1.1 hours of elapsed test time make it difficult to determine whether the outlet polyurethane manifold would have reached freezing significantly sooner than the inlet polyurethane manifold. The SWME outlet, outlet header water and polyurethane, and outlet-radially centered fiber temperature spikes combined with the vapor backpressure spike at 1.1 hours all suggest a slug of warm water reached the outlet side of the fiber cartridge. One explanation is a seal breach may have occurred at 1.1 hours allowing water to briefly squirt into the housing.

The water next to the outlet manifold turned into ice as evidenced by the  $-3^{\circ}\text{C}$  measured by the water thermocouple. It is interesting to note that the outlet water temperature reached freezing 2.3 minutes ahead of the adjacent polyurethane. The inlet water temperature remained above freezing throughout the test. Water breakthrough occurred 2.5 hours after valve closure initiation. It is not surprising the thawing of the SWME took longer than previous tests since significantly more water was frozen and the SWME was wrapped in MLI.

Once flow was re-established the freezing of the headers resulted in a profuse water leakage from the headers into the vacuum volume. Post-test analysis revealed that the seals had a manufacturing flaw (porosity) and a handling flaw (smooth cut) that were not detected before the test. These flaws may have been the site(s) of the putative coolant breach prior to the manifold freezing. A rough extension from the smooth cut handling flaw seems crack-like, with irregularities on the edge including a jagged turn indicative of overload. The opening of the smooth cut flaw likely acted a stress concentrator when the o-ring was subjected to loads during freezing conditions, leading to further cracking and tearing of the o-ring.<sup>9</sup> Once the o-rings were replaced the housing and the cartridge were retested and did not leak.

Loss of PLSS battery resulting in loss of pump and BPV motor power would result in frozen fibers, a recoverable condition. The crew would safely abort EVA using backup cooling system. But the extreme freeze produced by wrapping the SWME in multi-layer insulation in this test would probably not occur in flight, even with a battery failure, because the heat leak to the headers from internal PLSS radiation would significantly slow down the cooling rate in the headers.

#### D. Backpressure Valve Characterization

The first set of results presented in Figure 9 is from the repeat test day in which the BPV was stepped down from a fully open position to a fully closed position. The data is plotted with respect to BPV position, which corresponds to a predetermined BPV valve throat area and, therefore, valve poppet linear travel. The 28 BPV positions were estimated positions derived from the goal to effect 30 W SWME heat rejection changes from one position to the next. The average delta heat rejection ranged from 15 to 48 W with the average equal to 30 W when excluding the delta heat rejections of 0, 6, and 130 W at the BPV positions of 0, 1, and 27. The small delta heat rejections at the low BPV positions are attributable to the fact that the valve was almost completely closed and the additional motor stepping resulted in mostly valve poppet wave spring compression, not further travel of the valve poppet. At the high BPV positions, the number of motor steps selected proved to be too high to yield the goal of 30 W delta heat rejections.

Sensitivity to valve poppet travel is illustrated in **Error! Reference source not found.** by the box intersecting the 25% valve poppet travel point and also by the dashed lines marking 293 W SWME heat rejection. Opening the valve 25% resulted in a SWME heat rejection of 66% of its full open BPV value with the last 75% of valve poppet travel accounting for the final 34% of SWME heat rejection capability. The 293 W SWME heat rejection point serves as a proxy for total PLSS

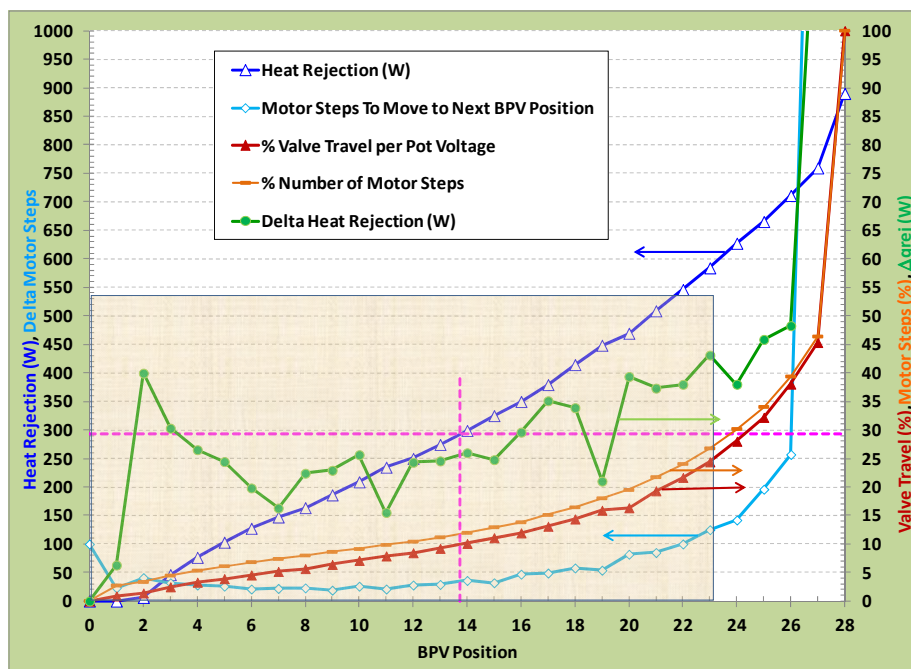


Figure 9. Backpressure Valve Characterization

Thermal Loop heat load for a moderate crew metabolic rate of 293 W (1000 Btu/hr), a very common metabolic rate during Lunar, Shuttle and ISS EVAs. Valve poppet travel at this point is 10% of the total valve poppet travel. SWME delta heat rejections of ~25 W about this point required 30 to 40 motor steps, 0.8 to 1.1% of the fully open BPV 3670 motor step count. As indicated by the results in **Error! Reference source not found.**, precise SWME heat rejection control requires precise valve travel control. The motor selected for this BPV with its 0.00305 mm valve stem travel per step (0.00012 in/step) met this goal.

### E. Utilization

The utilization is a measure of efficiency and is equal to the ratio of water consumption calculated from measured heat rejection to independent mass measurements of water used. The calculated water consumption is the SWME heat rejection integrated with respect to time and then divided by the water latent heat of vaporization to yield the apparent mass of water evaporated. Water usage was monitored throughout the entire test using a precision scale mounted under the feedwater supply tank. Ideally the SWME utilization is 1 which would show that all water consumed resulted in measured heat rejection. At times Utilization exceeded 1 due to instrumentation uncertainty.

Utilization was measured over the course of entire test days, typically 7 hours duration per day, over the span of 7 weeks (see Fig. 10). The utilization results ranged from 0.957 to 1.011, and have a average of  $0.987 \pm 0.017$ . The baseline heat rejection performance was an important standard of long duration performance (see Fig. 7). During baseline performance measurements the BPV was fully open and the SWME outlet temperature was controlled to 10 °C. While the baseline performance varied considerably throughout testing, the utilization of the same test points did not vary as much, and there was no obvious correlation between baseline performance and utilization. The utilization of the baseline performance ranged between 0.887 and 1.139, with an average of  $0.993 \pm 0.046$  (see Fig. 11). Two of the test points were uncharacteristically high (beginning of 5-May) and low (beginning of 26-Apr).

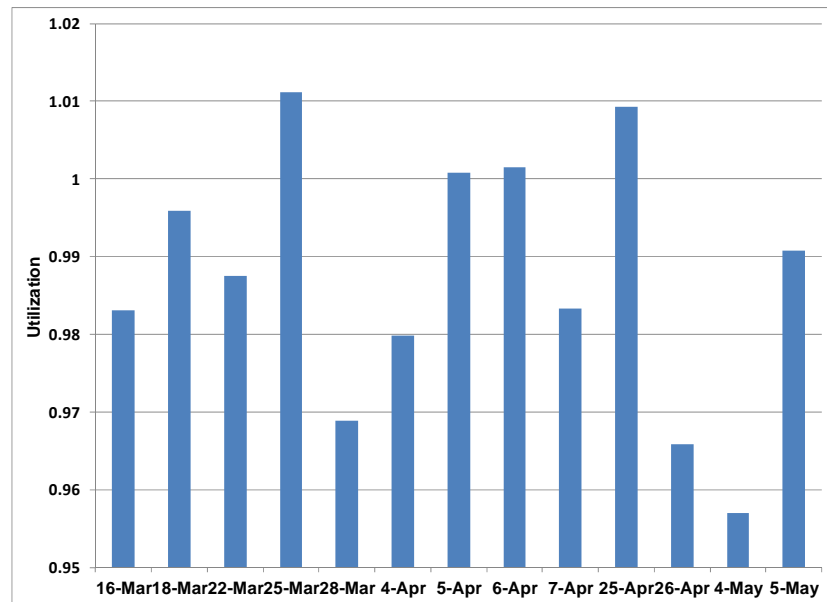


Figure 10. Full Day Utilization

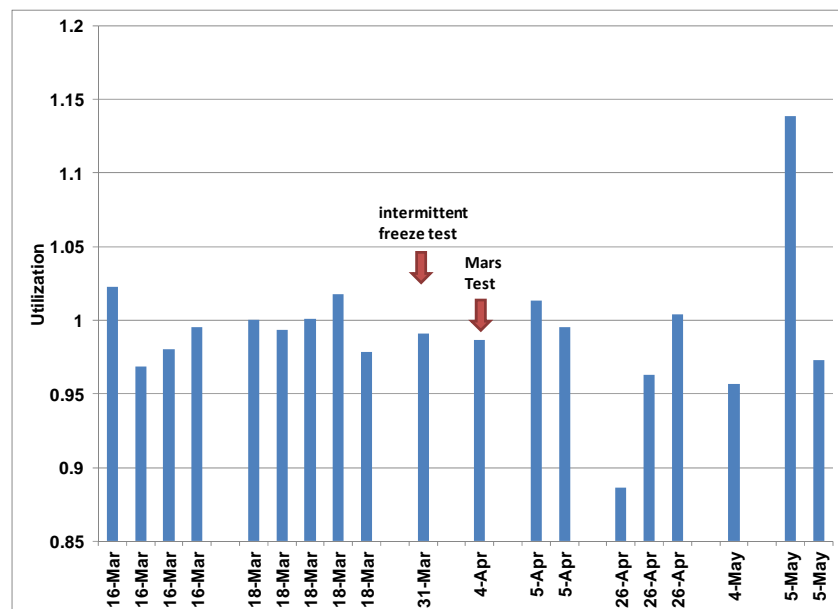
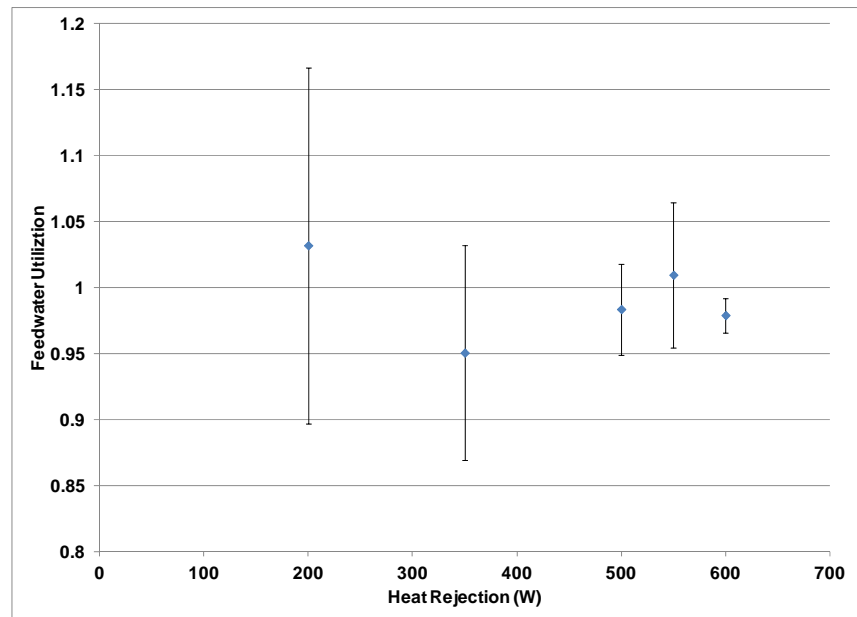


Figure 11. Baseline Performance Utilization

These may have been due to experimental error. If these are discarded, range is 0.963 to 1.023 with an average of  $0.991 \pm 0.019$ , which is very similar to the full day utilization measurements.

Utilization was also measured as a function of heat rejection rate for 22 test points, each with a duration of about 20 minutes (see Fig. 12). These average utilizations ranged from 0.951 to 1.032. The lower heat rejection rates, 200 W and 350 W had more variability than the higher heat rejection rates. This may be due to increased sensitivity to heat leak in and out of the system at lower heat rejection rates.

Utilization was also measured at different inlet temperature ranging from 16 °C to 36 °C, and at different flowrates, but with similar results to previous testing. There was no obvious relationship between inlet temperature and utilization or between flow rate and utilization. SWME utilization on average is within 2% of 1.0, and is not strongly influenced by cartridge cycle time, heat rejection rate, inlet temperature or flow rate. This is an expected result because at no time were ice chips observed in or around the SWME.



**Figure 12. Utilization for different heat rejection rates**

## V. Conclusions and Forward Work

SWME is a robust, compact, contamination resistant heat rejection device for advanced spacesuits. It has a utilization that on average is greater than 0.98 for all conditions studied. It has an effective and compact back pressure valve that provides effective control of heat rejection. SWME is freeze tolerant, but to avoid possible freeze damage, the SWME housing should not be insulated from the PLSS interior. SWME long duration performance proved to be variable and appeared to degrade from 800 W initially to about 700 W after six months and 600 hours of test operation. This degradation was apparently due to corrosion contamination, or biofilm or both. During this time the SWME apparently lost some hydrophobicity which was observed in loss of de-bubbling capability and weeping through the membrane. This performance instability and degradation may be controlled through use of corrosion resistant materials in the test loop and control of water quality through biocide and management of circulation loop constituents. The control of biofilm, water quality and corrosion resistant materials are the subject of an ongoing investigation which is the subject of a companion paper.<sup>x</sup>

## References

- <sup>1</sup>Bue G.; Makinen J., Vogel M., Honas M., Dillon P., Colunga A., Truong L., Porwitz D., and Tsioulos G., "Hollow Fiber Flight Prototype Spacesuit Water Membrane Evaporator Design and Testing" AIAA-2011-5259, 41st International Conference on Environmental Systems, Portland, Oregon, July, 2011.
- <sup>2</sup>Vogel M., "Generation 2 Hollow Fiber Spacesuit Water Membrane Evaporator Test Report" Jacobs Engineering memorandum, ESCG-4470-11-TEAN-DOC-0053, 30 September 2011.
- <sup>3</sup>Bue, G. C., Trevino, L. A., Hanford, A. J., and Mitchell, K., "Hollow Fiber Space Suit Water Membrane Evaporator Development for Lunar Missions," *International Conference on Environmental Systems (ICES)*, SAE International, 2009.
- <sup>4</sup>Bue, G. C., Trevino, L. A., Tsioulos, G., and Hanford, A., "Testing of Commercial Hollow Fiber Membranes for Spacesuit Water Membrane Evaporator," *International Conference on Environmental Systems (ICES)*, SAE International, 2009.
- <sup>5</sup>Vogel M., Vonau W., Trevino L., and Bue G., "Sheet Membrane Spacesuit Water Membrane Evaporator Design and Thermal Tests," AIAA-2010-6039, 40th International Conference on Environmental Systems, Barcelona, Spain, July 2010.

<sup>6</sup>Bue G.; Trevino L., Tsioulos G., Settles J., Colunga A., Vogel M., and Vonau W., “Hollow Fiber Spacesuit Water Membrane Evaporator Development and Testing for Advanced Spacesuits,” AIAA-2010-6040, 40th International Conference on Environmental Systems, Barcelona, Spain, July, 2010.

<sup>7</sup>Vonau Jr., W., Vogel, M., Conger, B., Hanford, T., Zapata, F. Mitchell, K. Dillon, P., and Frodge, C. “Sheet Membrane and Hollow Fiber Spacesuit Water Membrane Evaporators Test Report,” ESCG-4470-10-TEAN-DOC-0016, Engineering Sciences Contract Group, 2010.

<sup>8</sup>Steele J.; Rector T., Bue G., Campbell C., Makinen J. “Design and Evaluation of a Water Recirculation Loop Maintenance Device for the Advanced Spacesuit Water Membrane Evaporator” Submitted for publication, 42nd International Conference on Environmental Systems, San Diego, California, July, 2012.

<sup>9</sup>Tapia, A. S, “SWME-Spacesuit Water Membrane Evaporator Failure Analysis”, ES4-11-XXX, September 26, 2011.